Available online at www.sciencedirect.com
ScienceDirect
Polymer 48 (2007) 3530–3539
polymer
www.elsevier.com/locate/polymer

Study of the morphology of poly(butylene succinate)/poly(ethylene oxide) blends using hot-stage atomic force microscopy

Haijun Wang [a], Jerold M. Schultz [b,*], Shouke Yan [a]

[a] State Key Laboratory of Polymer Physics and Chemistry, Institute of Chemistry, The Chinese Academy of Sciences, Beijing 100080, China
[b] Department of Materials Science and Engineering, University of Delaware, Newark, DE 19716, United States

Received 21 December 2006; received in revised form 25 March 2007; accepted 30 March 2007
Available online 18 April 2007

Abstract

Blends of poly(butylene succinate) (PBS) and poly(ethylene oxide) (PEO) were cast into films, melted, and crystallized. A number of PBS/PEO blend compositions, ranging from 85/15 to 20/80 were used. The PBS, with a higher melting point, always crystallizes first, providing a scaffold on which the PEO would crystallize. AFM phase and height images were made at room temperature and at higher temperatures, as the PEO melted, allowing one to determine the morphology and location of the PEO. It was found that at low PEO concentrations (below 15 w/o) the PEO resides preferentially between PBS lamellae. This interlamellar PEO does not crystallize, except under extreme undercooling. At higher concentrations, larger amorphous domains exist within the PBS crystalline scaffold and PEO can crystallize in these domains. Two unexpected phenomena are observed: (1) the reversible exuding of PEO from interlamellar spaces to the surface for crystallization and (2) an unusual orientation of PEO lamellae within amorphous domains in the PBS scaffold.

Keywords: Blends; Crystallization; AFM

1. Introduction

Tailoring high-value polymers to produce optimal properties for specific applications has become increasingly important in polymer science and engineering. In the last decade, attention has focused significantly on polymer blends, engineering the composition and processing conditions to achieve a large inventory of morphologies and associating these with end uses.

Even more recently, the situation in which one (or more) of the constituents of the blend is crystallizable has been investigated. For such systems, an even wider range of morphologies has been opened. In these cases, the crystallization is often confined to, or initiated in, relatively small spaces. In fact, for such systems, it is the occurrence of liquid–solid phase separation that offers an effective route to produce a wide variety of morphological patterns [1]. An example would be an A/B blend system which is miscible in the melt and in which the melting point of component A is higher than that of component B. When A crystallizes at a temperature higher than the melting point of B, B acts as temporary amorphous diluent. The morphological pattern of this blend system is determined by the distance over which the component B diluent is expelled, where three basic types of separation may be generated: interlamellar segregation, interfibrillar segregation, or interspherulitic segregation. These morphological patterns represent the diluent dispersion from the nanometer scale for interlamellar segregation to the micrometer scale for interspherulitic segregation [2]. When the temperature is below the melting point of component B, B can then crystallize in any of the following modes: as another set of spherulites, in the spaces between first-formed spherulites, between growth arms in the first-formed spherulites, or between crystallites of the first-formed spherulites. A final possibility is cocrystallization of the two species, if the components are sufficiently similar.

* Corresponding author. Tel.: +1 302 235 7182; fax: +1 302 831 1048.
E-mail address: schultz@udel.edu (J.M. Schultz).

0032-3861/$ - see front matter © 2007 Elsevier Ltd. All rights reserved.
doi:10.1016/j.polymer.2007.03.079

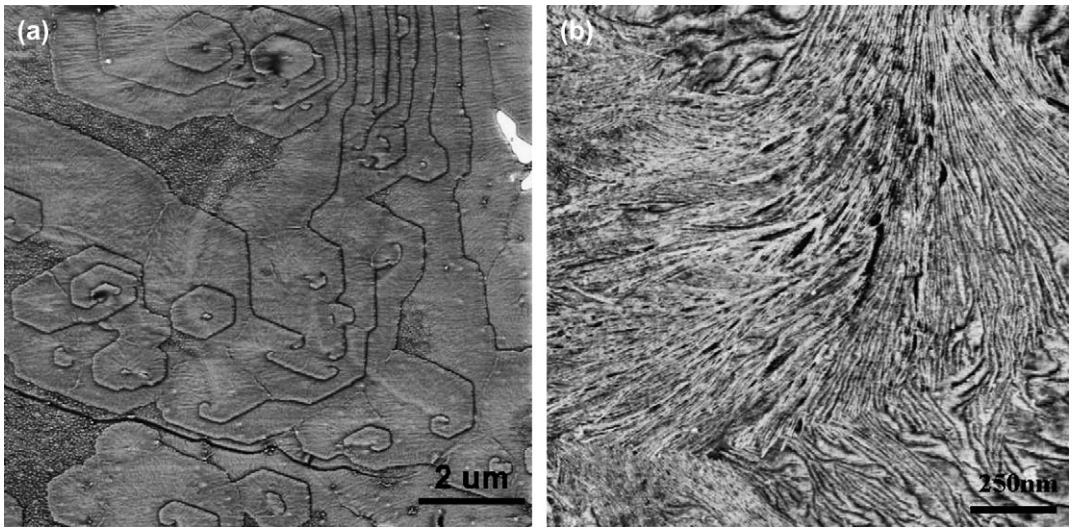

Fig. 1. Morphology of neat PBS using AFM phase contrast. In (a) the sample was heat-treated at 130 °C for 5 min and then isothermally crystallized at 100 °C. In (b) the sample crystallized during cooling to 0 °C at 30 °C/min. The scanning temperature on the AFM hot stage was 25 °C.

Many crystalline/crystalline blends such as polycarbonate (PC)/polycaprolactone (PCL) [3–6], poly(vinylidene fluoride) (PVDF)/poly(butylene adipate) (PBA) [7–11], poly(3-hydroxybutyrate) (PHB)/poly(ethylene oxide) (PEO) [12–14], poly(ethylene succinate) (PES)/PEO [2], PBT/polyarylates (PAr) [15], poly(vinylidene fluoride) (PVDF)/poly(3-hydroxybutyrate) (PHB) [16–18], and poly(butylene succinate) (PBS)/PEO [19,20] have been reported. PC/PCL, PVDF/PBA, PES/PEO, and PBS/PEO are systems whose morphological structures have been characterized at the lamellar level. It is to be noted that much of the evidence toward the site and morphology of the crystallization in such blend systems comes from scattering and fairly rudimentary microscopy studies. However, there is little information from controlled scanning probe microscopy or careful transmission electron microscopy.

The PBS/PEO blend system has been studied recently by He et al. [19,20]. The present contribution is instructed by He et al., and is a follow-on to that work. In that context, it is useful to review appropriate portions of He et al. [19,20]. In this system, the PBS normally crystallizes first, and the PEO later. In their first paper, they applied differential scanning calorimetry (DSC) and wide- and small-angle X-ray scattering (WAXS and SAXS) to a rather complete range of blends, to study the structures obtained during and following cooling at 10 °C/min from the melt (150 °C). During cooling, DSC traces showed clearly that there is a transition in PEO crystallization behavior above and below the PBS/PEO 70/30 composition. Below this composition, PEO crystallizes in the range 35–40 °C; above this composition, PEO crystallizes in the −10 °C to +5 °C range. The 70/30 blend exhibits both exotherms during cooling. In the dilute PEO regime (80/20 and above), comparing the crystallinity within lamellar stacks (using SAXS) with the macroscopic degree of crystallization, the authors find that the two quantities are identical. They conclude from this that the PEO crystallites reside between pre-existing PBS lamellae. From a similar comparison, they conclude that for PBS/PEO blends increasingly richer in PEO (increasingly lower than 80/20), more crystallization seems to take place between growth arms. However, there is no direct microscopic evidence for the location of the second-formed (PEO) crystals. In their subsequent paper [20], He et al. perform an interesting variant of the thermal history, pausing at a temperature T_I for 60 min before continuing to decrease the temperature to −50 °C. This enables the PBS component to crystallize isothermally at any temperature T_I, between 68 °C and 100 °C. It was found for all blend compositions below 25/75 that crystallizing PEO at sufficiently high temperatures T_I produces the low temperature PEO crystallization phenomenon. The temperature T_I necessary to produce this behavior increases with increasing PEO content. Using a combination of diffraction and macroscopic degree of crystallinity, they conclude that the blend composition and the crystallization temperature of PBS component have a large effect on the crystallization behavior and local distribution of the PEO component. In this case, as in all other similar blends, there has been little or no microscopy performed to directly verify the morphological conclusions. It is this evidence that we hope to supply, using atomic force microscopy (AFM) of crystallizing and crystallized PBS/PEO blend systems. In this article, we will map the crystal location and morphology in PBS/PEO blends over a range of compositions and crystallization temperatures.

2. Experimental

PEO ($M_w = 100{,}000$ g/mol) and PBS ($M_w = 200{,}000$ g/mol, $M_w/M_n = 1.1$) were both obtained from Aldrich Chemical. The melting points of PEO and PBS are measured to be 65 °C and 114 °C, respectively. Before use, PBS and PEO were purified by precipitation, respectively, into ethanol and *n*-hexane from chloroform solutions. Blends of PBS and PEO were prepared by solution blending with chloroform as a common solvent. Both of them were dissolved in chloroform with desired mass proportions (total polymer concentration

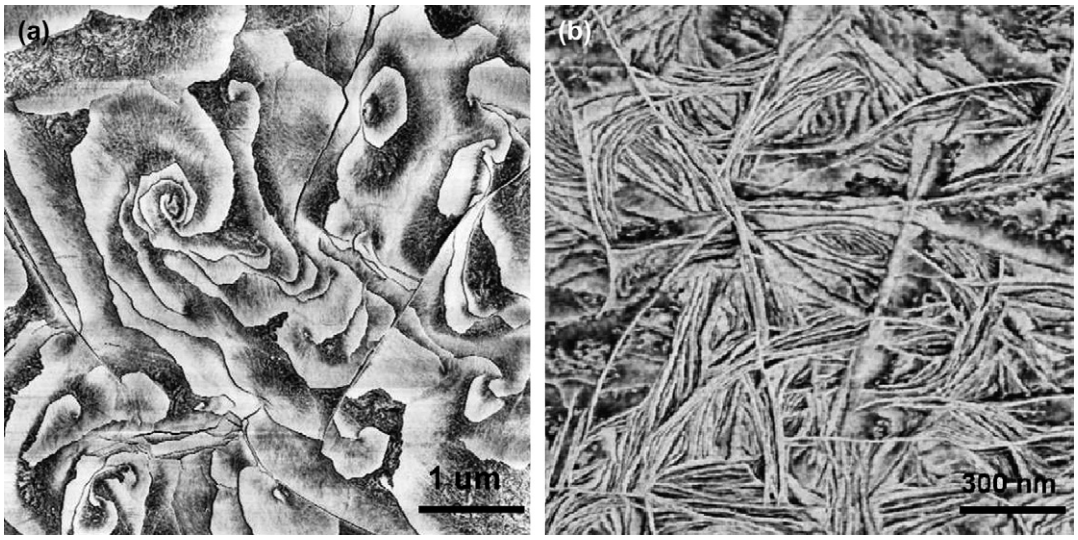

Fig. 2. Morphology of neat PBS using AFM phase contrast: (a) crystallized isothermally at 90 °C, (b) crystallized isothermally at 65 °C. Scanned at 25 °C.

was 10 mg/mL). The films for the AFM experiments were obtained by dip-coating onto a freshly-cleaved mica substrate, producing films 300 ± 10 nm in thickness. Some of the films were first melted at 130 °C for 3 min to erase previous thermal

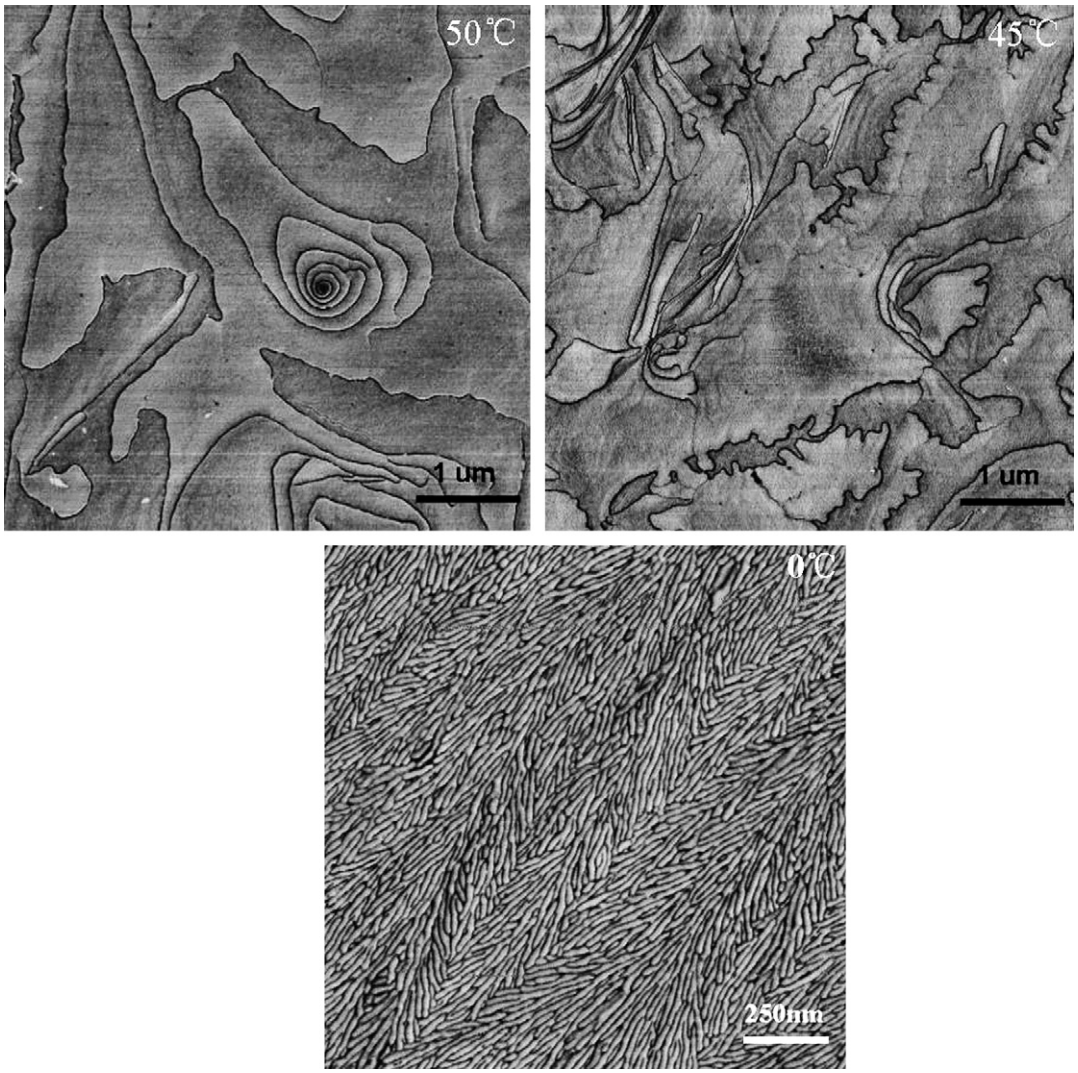

Fig. 3. AFM phase images of neat PEO, crystallized isothermally at the temperatures indicated. Scanned at 25 °C.

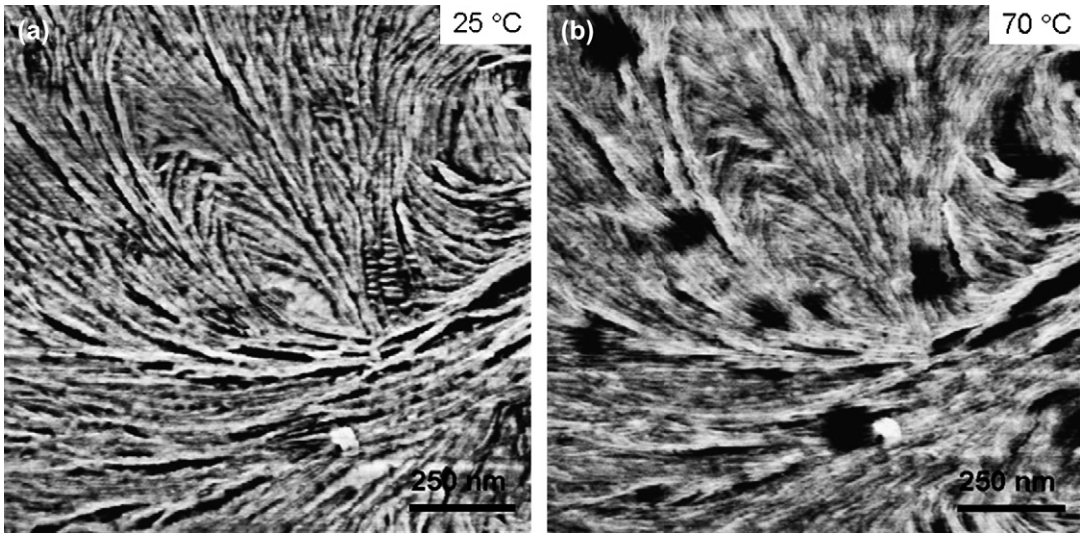

Fig. 4. AFM phase images of the same area of an 85/15 PBS/PEO blend which had been cooled to 0 °C at 30 °C/min. In (a) the image was scanned at 25 °C, in (b) at 70 °C.

history, then rapidly transferred to a second hot stage set at the desired crystallization temperature of the PBS component, and finally quenched to 0 °C for the crystallization of PEO. Other films were prepared by cooling directly from 130 °C to 0 °C or −70 °C at 30 °C/min.

Tapping-mode AFM images were obtained using a Nano-Scope III MultiMode AFM (Digital Instruments) equipped with a high-temperature heater accessory (Digital Instruments). Si cantilever tips (TESP) with a resonance frequency of approximately 300 kHz and a spring constant of about 40 N m^{-1} were used. The scan rate varied from 0.5 to 1.0 Hz. The set-point amplitude ratio (*r*sp) A_{sp}/A_0 was adjusted to 0.7–0.9, where A_{sp} is the set-point amplitude and A_0 is the amplitude of the free oscillation. The set-point ratio and amplitude were chosen such that the surface was tracked while maintaining the necessary contrast in the phase images. During slow heating at a rate of 2 °C/min from room temperature to 70 °C, each AFM image was obtained after the sample had been kept 5 min at the corresponding temperature. The experimental details of high-temperature AFM can also be found elsewhere [21–24]. While in situ AFM observations during crystallization would be very useful, this was not possible, since the crystallization half-time was too small to include multiple scans. Therefore the above protocol for observing ''static'' specimens was employed.

3. Results

The following PBS/PEO blend compositions were examined: 85/15, 70/30, 60/40, 50/50, 40/60, 30/70 and 20/80. In all cases, material was cooled from the melt to crystallize both components. As described in Section 2, this was done sometimes in two stages, first crystallizing the PBS at a temperature above the melting point of PEO, and then cooling further to crystallize the PEO. Alternatively, both components were crystallized during continuous cooling. Following crystallization of the PEO, the surface of the material was examined by AFM at room temperature, and then at higher temperatures, especially temperatures above that at which the PEO had melted. In this way, it was possible to identify the morphological state of the PEO and to establish the loci of its crystals. Following a description of the morphological characteristics of the neat components, we will examine sequentially the results for each blend composition.

3.1. Neat PBS and PEO

In the study of PBS/PEO blends, PBS always crystallizes first, providing the scaffold on which PEO crystallizes. Conveniently, the PBS films of the thickness used here can be crystallized with the PBS platelets viewed either edge-on or face-on, depending on the temperature of crystallization. Fig. 1 shows PBS films (a) crystallized isothermally at 100 °C and (b) crystallized during cooling at 30 °C/min from 130 °C to 0 °C. After crystallizing at 100 °C the lamelliform crystals form in the plane of the film; they are seen face-on. After cooling to 0 °C from the melt, the crystal lamellae have their face normals in the plane of the film; they are seen edge-on. For isothermal crystallization below 100 °C, morphologies intermediate between these two extremes are found, as shown in Fig. 2. PBS crystallized isothermally at 90 °C exhibits a basically face-on morphology, but the lamellae growing about giant screw dislocations scroll away from the basic face-on orientation, forming characteristic flowerlike shapes. Material crystallized at 65 °C, on the other hand, exhibits a fundamentally edge-on orientation, but with crystals rotating also into a face-on orientation. We make no attempt here to explain why the different orientations and morphologies form; we merely use the opportunity to view at different lamellar orientations.

The situation for neat PEO is similar to that for PBS, as evidenced in Fig. 3. At small supercoolings, e.g., 50 °C, the

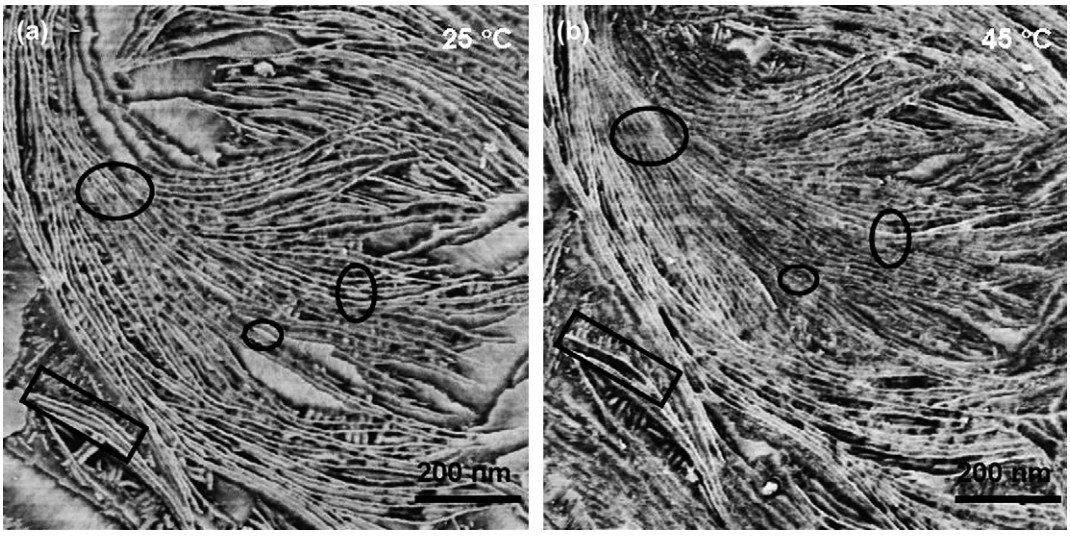

Fig. 5. AFM phase images of the same area of an 85/15 PBS/PEO blend. In this film, the PBS was crystallized at 70 °C (180 min) and then cooled to −70 °C at 30 °C/min. Images were scanned at (a) 25 °C and (b) 45 °C. Outlines indicate areas where interlamellar crystallization and melting of PEO can be seen.

lamellar normals are perpendicular to the plane of the film, while at large undercoolings (cooling to 0 °C), the lamellar normals lie preferentially in the film plane. In the example shown, the average lamellar width is 11.8 nm. Shown also in Fig. 3 is a film crystallized at 45 °C. Like the film crystallized at 50 °C, the crystalline lamellae are seen face-on, the main morphological

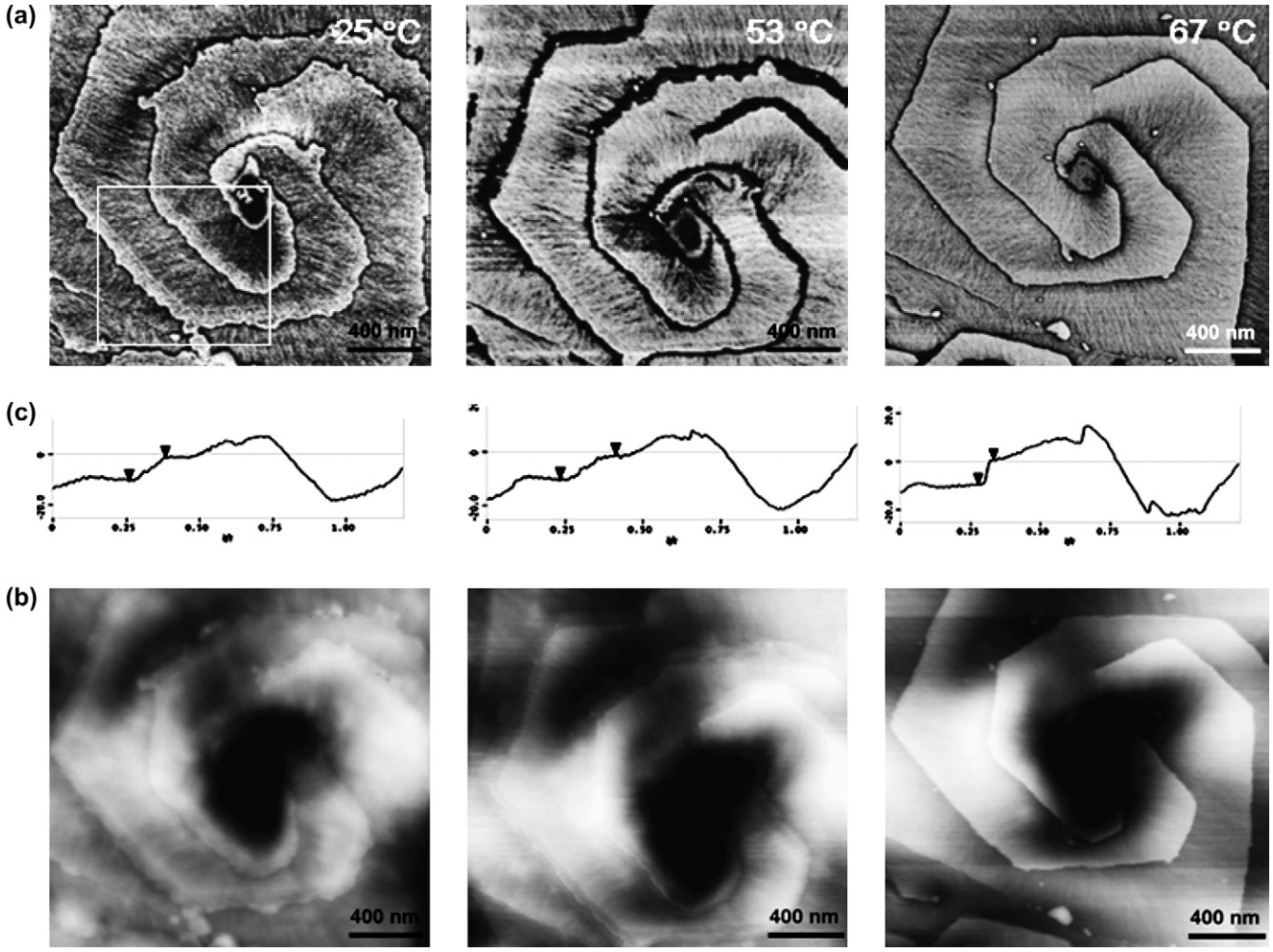

Fig. 6. AFM images ((a) phase and (b) height) of the same area of a 70/30 PBS/PEO blend. In this film, the PBS was crystallized at 95 °C (180 min) and the film then cooled to 0 °C at 30 °C/min. (c) Height traces from the lower left to near the center. The images were obtained at 25 °C, 53 °C and 67 °C.

difference being the breakdown of the growth front into stubby ''fingers''. The interfacial breakdown is likely in response to a self-generated compositional or stress field [25].

3.2. PBS/PEO 85/15

This is a blend in the dilute PEO range, for which the results of He et al. indicate that all the PEO must be interstitial between PBS lamellae, and that the PEO is not crystallized. The present results broadly support this finding. Fig. 4 shows a pair of AFM phase images, taken at room temperature (a) following continuous cooling to 0 °C and (b) the same area after holding at 70 °C. It is seen that patches of lamellae seen edge-on in (a) are not present in (b). From the appearance of the lamellae and their disappearance when PEO should melt, it is concluded that these are PEO crystals. It is not known whether these patches of PEO represent what occurs in the bulk or whether this is material exuded to the surface during PBS crystallization. What is known is that the PEO patches in this field constitute no more than 10% of the total area, a finding corroborated in two other areas. Further, examining the details of the image, crystal by crystal, one finds no melting of crystals within the edge-on stacks. These results show that (1) at least some of the PEO must lie between PBS lamellae (since the PEO at the surface is not at the bulk composition) and (2) the PEO within the PBS lamellar stacks is not crystalline.

It must be mentioned here that for these images and all the subsequent ones, we are examining the free surface which formed during crystallization. The extent to which these observations represent bulk behavior is not known. The specimen being fairly thin, it is likely that the initial morphology is representative, but the changes observed upon heat-treatment may be more specific to the free surface.

He et al. also noted that dilute blends subjected to a deeper quench gave evidence that at least some of the PEO had crystallized. Fig. 5 shows AFM phase images for PBS/PEO 85/15 material which was quenched to −70 °C prior to imaging at (a) room temperature and then (b) 45 °C. In (a) one sees PEO lamellae face-on covering a portion of the edge-on PBS lamellae. Again, one cannot tell whether these face-on

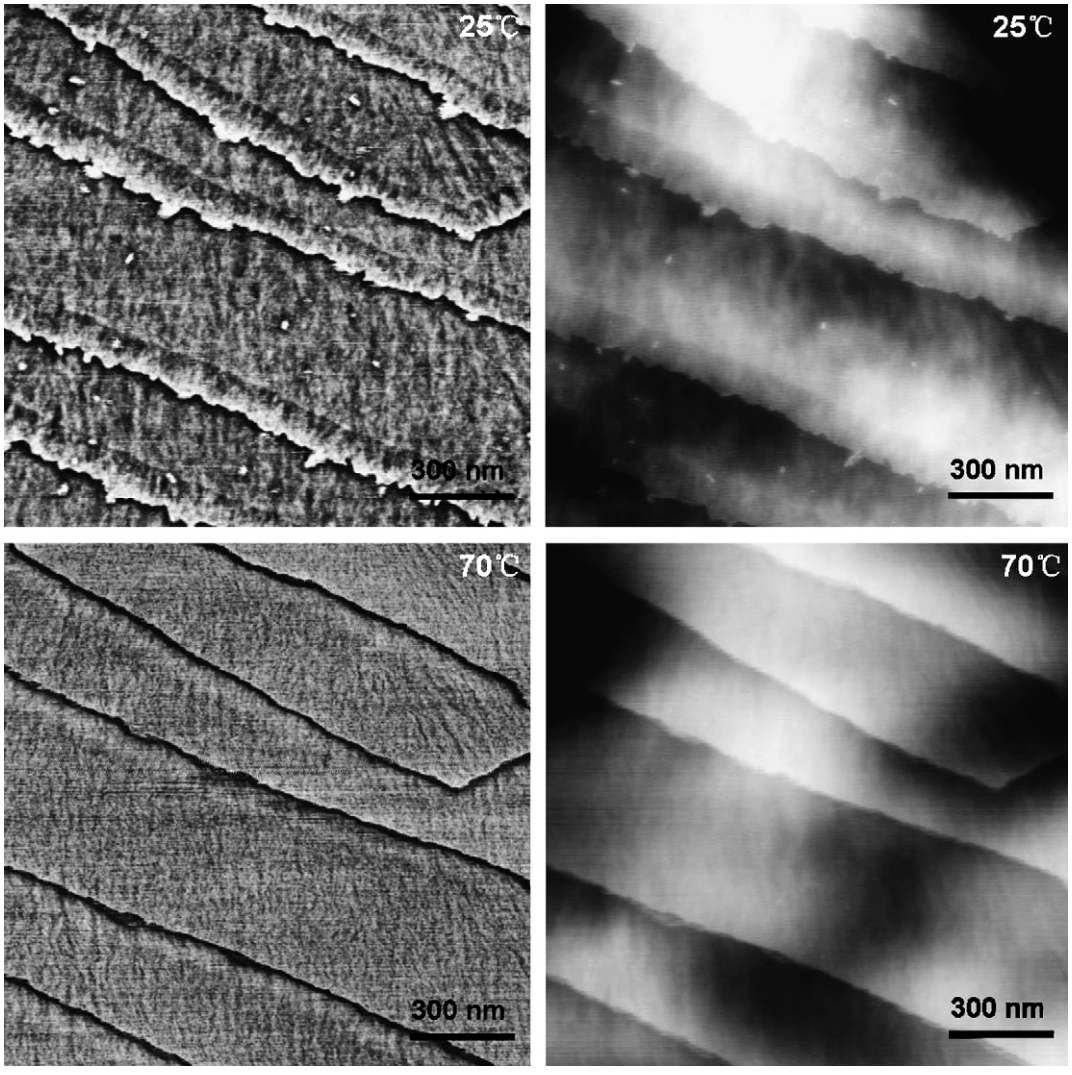

Fig. 7. AFM phase (left) and height (right) images of the same area of a 60/40 PBS/PEO blend. In this film, the PBS was crystallized at 95 °C (180 min) and then cooled to 0 °C at 30 °C/min. Images were scanned at 25 °C (top) and 70 °C (bottom).

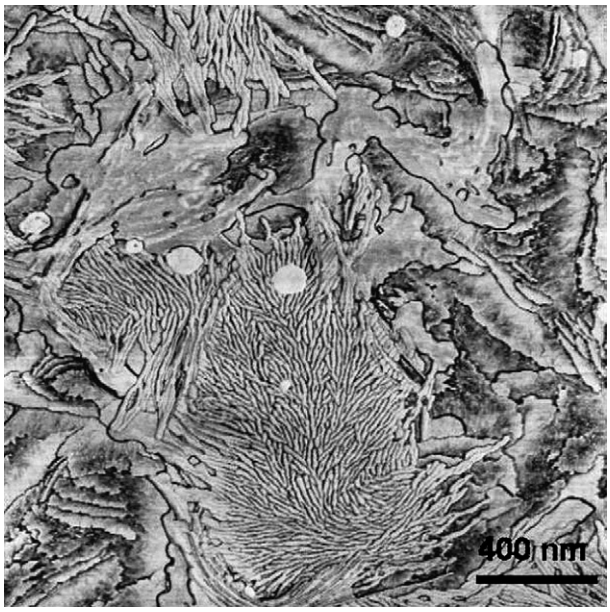

Fig. 8. AFM phase image of a 70/30 PBS/PEO blend which was cooled directly from the melt (130 °C) to 0 °C and then scanned at 25 °C.

PEO crystals represent the bulk or if they represent material exuded to the surface. More interestingly, occasional bright lamellae and extended ''dots'' are to be seen at room temperature, but not at 45 °C. These appear to be PEO crystals lying between PBS crystals. These PEO crystals are small and melt at a relatively low temperature, presumably because of capillarity. This area exhibits no further change upon increasing the temperature to 70 °C.

3.3. PBS/PEO 70/30 and 60/40

Fig. 6 shows AFM results for a 70/30 blend in which the PBS was isothermally crystallized at 95 °C prior to cooling the film to 0 °C. Fig. 6(a) and (b) shows phase and height images of a region containing a giant screw dislocation. Such a region is chosen because it is easily located when the temperature is changed and drift occurs. The height traces shown in Fig. 6(c) were taken from the lower left to the upper right of the boxes shown in Fig. 6(a). Beginning with the images and height trace at 67 °C, after melting the PEO, we see sharp-edged PBS lamellae. At room temperature the sharp PBS edges (seen faintly in the images) had been extended by a border of crystallized PEO. At 53 °C, approaching the melting point of PEO, the border is still there, but the outer rim of the border now appears to be molten, as indicated by the blackness of this rim in the phase image. The phase image of the PBS crystals at 67 °C also shows a narrow black rim about the crystals, suggesting the presence of softer material there, presumably molten PEO. The PEO borders in Fig. 6(a) represent 20% of the area. Other regions show not more than this level of PEO coverage. The remaining PEO is

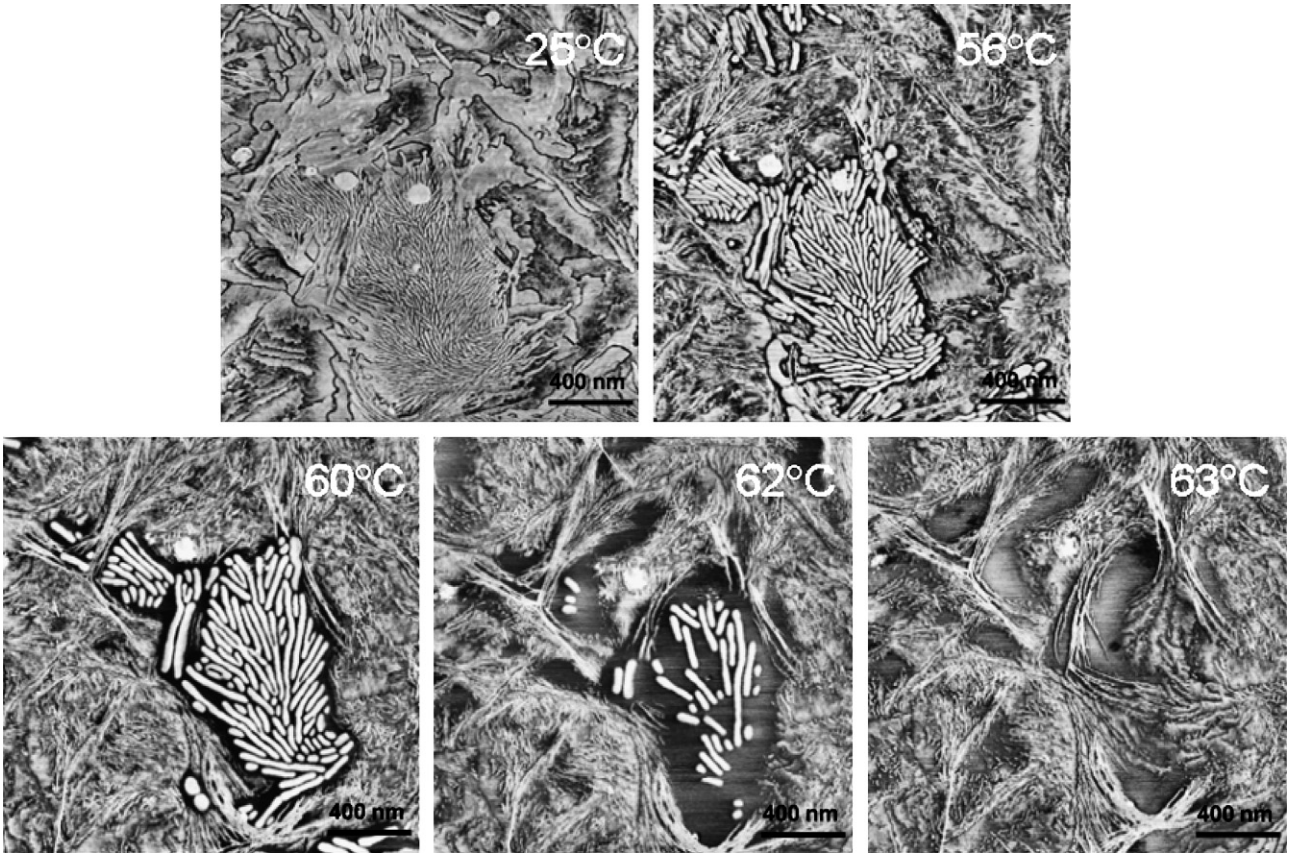

Fig. 9. AFM phase images of the area shown in Fig. 8 (60/40 PBS/PEO blend cooled directly from 130 °C to 0 °C). Images were scanned at the temperatures indicated.

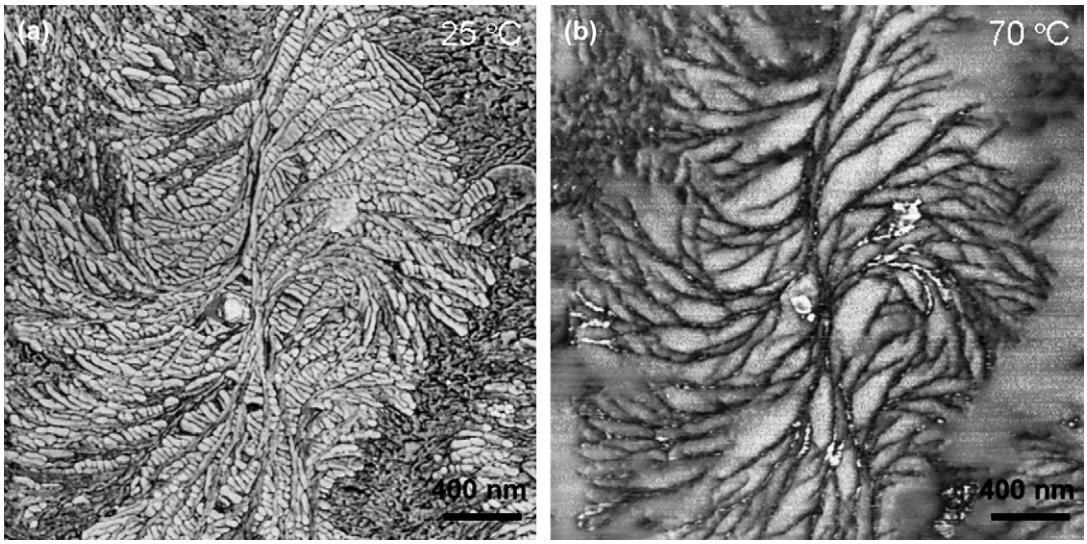

Fig. 10. AFM phase images of a 40/60 PBS/PEO blend in which the PBS was crystallized isothermally at 65 °C (180 min) and the specimen was then quenched to 0 °C and held there for 30 min. Images were scanned at (a) 25 °C and (b) 70 °C.

therefore below the surface, again likely between PBS lamellae. It is significant also that there is no trace of molten PEO in the image at 67 °C, either before or after lowering the temperature to crystallize the PEO. It would appear that the molten PEO has migrated into the region between PBS lamellae. This migration is likely driven either by capillarity or by mixing entropy.

PBS/PEO 60/40 films prepared by the same two-stage procedure (130 °C to 95 °C to 0 °C) show the same features as do the 70/30 films. An example is shown in Fig. 7. Again a PEO border on the PBS lamellae is seen at room temperature, but is absent at 70 °C. In the region shown, the crystalline PEO border covers 28% of the total area, significantly less than the overall composition. As was seen in the 70/30 films, there is little trace of molten PEO after melting has occurred, again indicating a retraction within the lamellar stack upon melting.

When films of the 70/30 composition are cooled directly from 130 °C to 0 °C, the PBS lamellae crystallize in the edge-on orientation, as shown in Fig. 1(b). The surface of the blend shows a predominant overlayer of face-on PEO, with occasional patches of edge-on PEO lamellae. An example showing both face-on and edge-on PEO lamellae is shown in Fig. 8. Fig. 9 shows what happens as the temperature of the film is raised from room temperature: the PEO overgrowth gradually melts, revealing the underlying edge-on PBS lamellae. It is seen that the location of the edge-on PEO lamellae identifies with large pockets among PBS lamellar stacks. This is common in more PEO-concentrated blends and will be described more fully below. Since the PBS substrate is initially obscured by the PEO overgrowth, there is little more to learn by following the melting behavior of the PEO.

3.4. PBS/PEO 60/40 to 20/80, with PBS crystallized at 65 °C

Blends having PBS/PEO ratios in the range 60/45 to 20/80 exhibit similar features when the PBS is crystallized isothermally at 65 °C before cooling further to 0 °C. One finds PEO crystallization within PBS scaffolds, as illustrated in Fig. 10 for a 40/60 blend. The highly branched native PBS scaffold can be seen at 70 °C, after the PEO has been melted. At room temperature, prior to melting, the PEO crystals bridge the large pockets between adjacent PBS branches, as seen in Fig. 10(a). Fig. 11 is an enlarged portion of Fig. 10(a). This enlargement shows the PEO crystals to be partially overlapped face-on lamellae. The PEO lamellae lie at a large angle to the PBS branches and are rather parallel to each other. Fig. 12 is another example of the same phenomena, this time for a 30/70 blend with the same thermal treatment. Here we see that even though the PEO lamellae sometimes bend toward the space available for crystallization, they have begun in a direction roughly normal to the basal surfaces of the PBS lamellae.

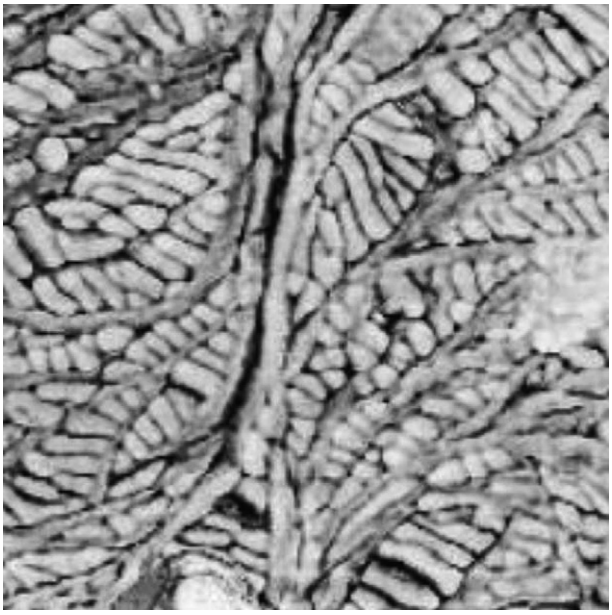

Fig. 11. Higher resolution image of a portion of Fig. 10(a).

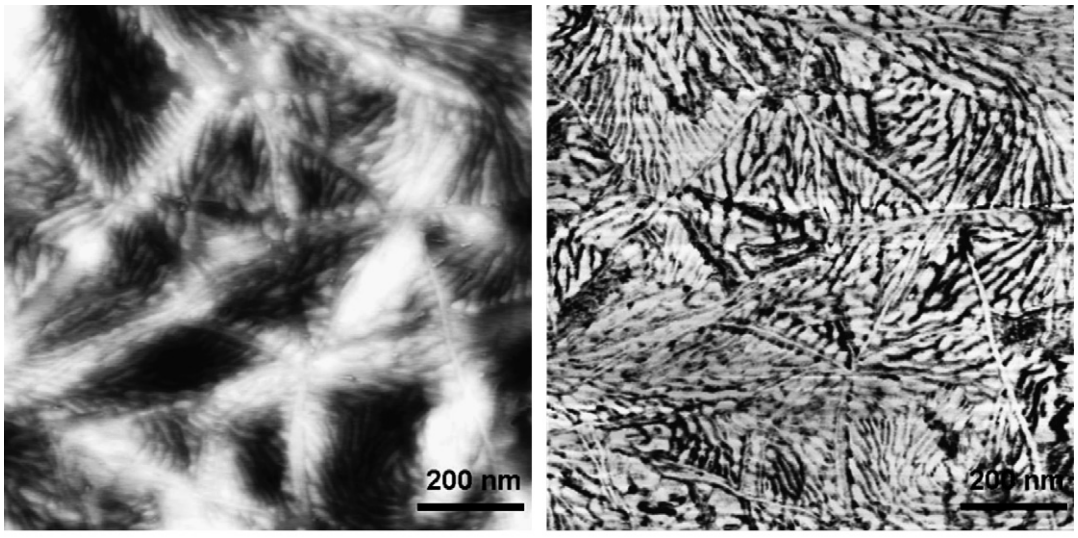

Fig. 12. AFM phase and height images of a PBS/PEO 30/70 blend which had been cooled directly from 130 °C to 0 °C and held at 0 °C for 30 min. Scanning was performed at 25 °C.

Two features are of interest here: the orientation of the PEO lamellae within the long and narrow interbranch pockets and the face-on orientation of the lamellae. Were the profuse PEO lamellae to have nucleated in random orientations within the pockets, the surviving lamellae would be preferentially oriented along the long direction of the pockets, as would be usual for lathlike crystals confined to grow in a channel [26]. It appears then that the orientation – approximately normal to the PBS lamellae – must be set at the nucleation event. The face-on orientation of the PEO crystals is also counter to what was reported above for neat PEO and PEO-poor blends. In those cases, PEO crystallized with the lamellar normals dominantly in the plane of the film (edge-on orientation). The unusual growth direction of the PEO lamellae within the narrow pockets and the unexpected orientation with respect to the film plane suggest that the PEO crystals nucleate epitaxially on the PBS crystals, and that the direction and orientation are dictated by the crystallography of the epitaxy.

4. Discussion

The above results relate to the disposition of PEO within the framework of already crystallized PBS. It was shown that the uncrystallized spaces within PBS lamellar stacks can retain PEO, up to a concentration of some 15% by weight. This result, and others in this study, correspond well with that of He et al. obtained largely from scattering studies [19,20], coupled with other data (a nice confirmation that scattering, combined with other results, can produce detailed morphological information). Further, most of the interlamellar PEO crystallizes only at very large undercooling (in the present work, quenching to −70 °C), indicating that such small spaces require very thin crystals, whose relatively large surface to volume ratio lowers the stability of the crystals. Above some 30 wt%, larger uncrystallized pockets are available in the PBS crystalline scaffold, and the PEO component preferentially crystallizes in these pockets.

The results at the PBS/PEO 70/30 composition are particularly intriguing. Evidence was shown that molten PEO can migrate to and from the PBS interlamellar space, migrating outward to crystallize and inward after melting. The outward migration is likely propelled by the ability to form, on the surface, crystal lamellae thicker than is possible in the narrow interlamellar space. It is not until larger molten spaces become available in blends of higher PEO concentration (PBS/PEO 60/40 and lower) that PEO can crystallize massively in the PBS scaffold. The retraction of the molten PEO into the interlamellar space could be driven either by the entropy of mixing or by favorable surface energy.

5. Conclusions

The following conclusions are drawn from the results of this study.

1. The conclusions of He et al. [19,20], regarding the disposition of PEO crystals within the existing PBS scaffold are borne out.
2. At low (<15 w/o) PEO concentrations, PEO resides predominantly in the interlamellar spaces in the PBS scaffold. Much of the PEO is uncrystallized, unless driven by extreme undercooling.
3. At larger PEO concentrations (>30 w/o) PEO crystallites are found in the large noncrystalline pockets between PBS growth arms.
4. In blends containing 30 w/o PEO, PEO is exuded from PBS interlamellar spaces to the surface, where it crystallizes at the edges of the existing PBS lamellae. It appears that only at the surface can the PEO crystallize at stable thicknesses. Upon melting, the molten PEO retreats to the PBS interlamellar spaces.

5. Preferred orientations of PEO crystals in PBS interarm pockets indicate epitaxial control.

Acknowledgements

The financial support of the Outstanding Youth Fund (No. 20425414) and the National Natural Science Foundations of China (No. 50521302, 20574079 and 20634050) is gratefully acknowledged.

References

[1] Stein RS, Khambatta FB, Warner FP, Russell T, Escala A, Balizer E. J Polym Sci Polym Symp 1978;63:313.
[2] Chen HL, Wang SF. Polymer 2000;41:5157.
[3] Cheung YW, Stein RS, Wignall GD. Macromolecules 1993;26:5365.
[4] Cheung YW, Stein RS. Macromolecules 1994;27:2512.
[5] Cheung YW, Stein RS, Chu B, Wu G. Macromolecules 1994;27:3589.
[6] Cheung YW, Stein RS, Lin JS, Wignall GD. Macromolecules 1994;27:2520.
[7] Penning JP, Manley RStJ. Macromolecules 1996;29:77.
[8] Penning JP, Manley RStJ. Macromolecules 1996;29:84.
[9] Fujita K, Kyu T, Manley RStJ. Macromolecules 1996;29:91.
[10] Liu LZ, Chu B, Penning JP, Manley RStJ. Macromolecules 1997;30:4398.
[11] Liu LZ, Chu B, Penning JP, Manley RStJ. J Polym Sci Part B Polym Phys 2000;38:2296.
[12] Avella M, Martuscelli E. Polymer 1988;29:1731.
[13] Avella M, Martuscelli E, Greco P. Polymer 1991;32:1647.
[14] Avella M, Martuscelli E, Raimo M. Polymer 1993;34:3234.
[15] Liu AS, Liau WB, Chiu WY. Macromolecules 1998;31:6593.
[16] Liu JP, Jungnickel BJ. J Polym Sci Part B Polym Phys 2003;41:873.
[17] Liu JP, Jungnickel BJ. J Polym Sci Part B Polym Phys 2004;42:974.
[18] Chiu HJ, Chen HL, Lin JS. Polymer 2001;42:5749.
[19] He Y, Zhu B, Kai WH, Inoue Y. Macromolecules 2004;37:3337.
[20] He Y, Zhu B, Kai WH, Inoue Y. Macromolecules 2004;37:8050.
[21] Jiang Y, Yan DD, Gao X, Han CC, Jin XG, Li L. Macromolecules 2003;36:3652.
[22] Hobbs JK, McMaster TJ, Miles MJ, Barham PJ. Polymer 1998;39:2437.
[23] Schultz JM, Miles MJ. J Polym Sci Part B Polym Phys 1998;36:2311.
[24] Ivanov DA, Amalou Z, Magonov SN. Macromolecules 2001;34:8944.
[25] Schultz JM. Polymer crystallization. Oxford, U.K.: Oxford University Press; 2001. p. 199.
[26] Schultz JM. J Polym Sci Polym Phys Ed 1992;30:785.